1D Slipped Stacking Microribbon -like Crystals Based on 6,13 -Dicyanopentacene for Ambipolar Charge Transport

Zongrui Wang[a*]†, Yang Hu[a]†, Yujie Xie[a]†, Fengxiang Qie[b], Junfeng Guo[a,c], Lei Zhang[a], Chunfeng Shi[b*], Florian Glöcklhofer[d*], Yonggang Zhen[a,e*]

ABSTRACT Featuring small charge transport scattering, mesoscale size, and easy fabrication, one-dimensional self-assembled micro/nanomaterials (1D-MNMs) based on organic π-conjugated systems can be facilely incorporated into integrated microcircuits. Although tremendous progress has been made in 1D-MNMs based on p- or n-channel organic semiconductors, examples of 1D-MNMs based on ambipolar organic semiconductors are scarce. Herein, we achieved a novel 1D-MNM based on 6,13-dicyanopentacene (DCP) with a 1D slipped stacking motif using the physical vapor transport method. The DCP-based 1D-MNM showed outstanding, well-balanced ambipolar charge transport with electron and hole mobilities of up to 0.34 and 0.38 $cm^2 V^{-1} s^{-1}$, respectively, which are among the best ambipolar transport characteristics of 1D-MNMs. Furthermore, a complementary inverter based on the ambipolar 1D-MNM of DCP is also constructed with a gain of up to 7, indicating potential application in organic logic circuits.

Keywords: 1D slipped stacking, micro/nanomaterials, ambipolar charge transport, complementary inverter

INTRODUCTION

The last several decades have witnessed rapid development in one-dimensional self-assembled micro/nanomaterials (1D-MNMs) based on organic π-conjugated systems because of their facile incorporation into integrated microcircuits with less scattering of charge transport, mesoscale size, and easy fabrication [1-5]. Generally, 1D slipped stacking and parallel face-to-face columnar packing are two major motifs to specifically induce 1D-MNMs wherein the π–π intermolecular contacts predominate [6]. Although tremendous progress has been made in 1D-MNMs based on p- or n-channel organic semiconductors [1, 6-13], examples of 1D-MNMs based on ambipolar organic semiconductors are scarce. Furthermore, low and unbalanced hole and electron charge transport is a major long-standing issue for ambipolar organic semiconductors, hindering the development of ambipolar transistors, which, therefore, usually require micropatterning of the individual p- and n-channel semiconductors [14-17]. In terms of molecular design, two strategies are used to tailor the frontier molecular orbitals toward ambipolar organic semiconductors: combining an electron donor and acceptor into a new molecular system [18] and introducing electron-withdrawing groups such as fluorine/chlorine/nitrogen atoms, trifluoromethyl, or cyano units on the π-conjugated backbone of p-type semiconductors [14, 16-17, 19-21].

Pentacene is one of the most extensively studied p-type semiconductors in organic field-effect transistors, showing a ultrahigh hole mobility of up to 40 $cm^2 V^{-1} s^{-1}$ [22]. Given this outstanding charge transport behavior, much effort has been dedicated to the chemical modification of pentacene to open additional electron transport by lowering the lowest unoccupied molecular orbital (LUMO) level [14, 16, 19-20]. For example, Bao et al. achieved a series of ambipolar halogenated pentacene derivatives by controlling the number of electron-withdrawing halogens (such

[a] Advanced Innovation Center for Soft Matter Science and Engineering, State Key Laboratory of Organic-Inorganic Composites, Beijing University of Chemical Technology, Beijing, 100029, China
[b] State Key Laboratory of Catalytic Materials and Reaction Engineering, Research Institute of Petroleum Processing, SINOPEC, No. 18 Xueyuan Road, Beijing 100083, China
[c] StateKey Laboratory of Luminescent Materials and Devices, South China University of Technology, Guangzhou 510640, China
[d] Department of Chemistry and Centre for Processable Electronics, Imperial College London, London, W12 0BZ, United Kingdom
[e] State Key Laboratory of Optoelectronic Materials and Technologies, Sun Yat-sen University, Guangzhou 510275, China
† These authors contributed equally
* Corresponding author (email: wangzr@buct.edu.cn; shicf.ripp@sinopec.com; f.glocklhofer@imperial.ac.uk; zhenyg@buct.edu.cn)

as F and Cl) at the pentacene core, wherein the compound containing eight fluorine atoms exhibited balanced ambipolar transport, with hole and electron mobilities of up to 0.51 and 0.46 $cm^2 V^{-1} s^{-1}$ under nitrogen, respectively [19]. Miao et al. introduced nitrogen heteroatoms on the pentacene skeleton, demonstrating ambipolar charge transport with electron and hole mobility of 1.1 and 0.07 $cm^2 V^{-1} s^{-1}$ in vacuum, respectively [14]. Zhang et al. synthesized the pentacene derivative 8,9,10,11-tetrachloro-6,13-bis-(triisopropylsilylethynyl)-1-azapentacene, which showed balanced ambipolar charge transport with a hole and electron mobility of 0.12 and 0.14 $cm^2 V^{-1} s^{-1}$ under nitrogen, respectively [16]. Despite these fruitful achievements in developing ambipolar transporting pentacene derivatives, studies have focused on thin films, wherein the grain boundaries and charge traps are the major obstacles to improving carrier mobility. To the best of our knowledge, no report is available on 1D-MNMs based on ambipolar transporting pentacene derivatives.

Previously, we introduced two cyano groups on the pentacene core to achieve an ambipolar semiconductor 6,13-dicyanopentacene (DCP) by a one-pot synthetic methodology [20, 23]. In virtue of the strong electron-withdrawing ability of cyano groups, the LUMO level was lowered considerably to facilitate the electron injection, thus leading to ambipolar charge transport characteristics (μ_e: ~10^{-4} $cm^2 V^{-1} s^{-1}$, μ_h: 10^{-3}–10^{-4} $cm^2 V^{-1} s^{-1}$) in thin-film devices [20, 24]. Very interestingly, we observed that introducing cyano substituents at the 6,13-positions of pentacene results in pronounced steric effects. In particular, it prevents the C-H···π interactions between adjacent molecules that lead to herringbone packing in the case of pentacene, and thus induces 1D slipped stacking controlled by π–π interactions. Because of the 1D slipped stacking motif, we anticipated that DCP is prone to growing 1D-MNMs. Herein, we successfully obtained microribbon-like single crystals of DCP using the physical vapor transport (PVT) method [25] and systematically investigated their charge transport characteristics in single-crystal field-effect transistors (SCFETs). Outstanding ambipolar charge transport was achieved, with balanced electron mobility of 0.34 $cm^2 V^{-1} s^{-1}$ and hole mobility of 0.38 $cm^2 V^{-1} s^{-1}$, which is among the best ambipolar carrier mobilities for 1D-MNMs. Furthermore, the relationship between molecular stacking, crystal growth, and charge transport characteristics has also been revealed. In addition, an inverter based on the ambipolar 1D-MNMs of DCP was also successfully fabricated, indicating a potential application in organic circuits [26-28].

RESULTS AND DISCUSSION

DCP (Figure 1a) was synthesized from 6,13-pentacenequinone in a single reaction, as previously reported [20, 23]. The frontier molecular orbital energy levels were determined from UV–*vis* absorption spectroscopy and cyclic voltammetry measurements (Table S1, ESI†) [20]. The low-lying LUMO level (−4.16 eV) and relatively narrow bandgap (1.62 eV) resulting from the introduction of the strong electron-withdrawing cyano groups suggest the possibility for ambipolar transport [29].

Single-crystal 1D-MNMs were prepared using the PVT method (Figure S1, ESI†) [25]. Specifically, DCP was placed in the heating zone of a furnace and heated at 200°C for 4 h under argon flow at a rate of 12 mL/min. In doing so, DCP slowly sublimated and then recrystallized on the surface of OTS (n-octadecyltrichlorosilane)-modified Si/SiO_2 substrates to form microribbon-like crystals in the cooling zone (Figure 1b). As displayed in Figure 1 and Figures S2 and S3, microcrystals grew on the substrate surface in two manners: a lying-down mode (Figure 1c, Figure S2b, Mode 1) and a standing-up mode (Figure 1d, Figure S2a, and Figure S3, Mode 2).

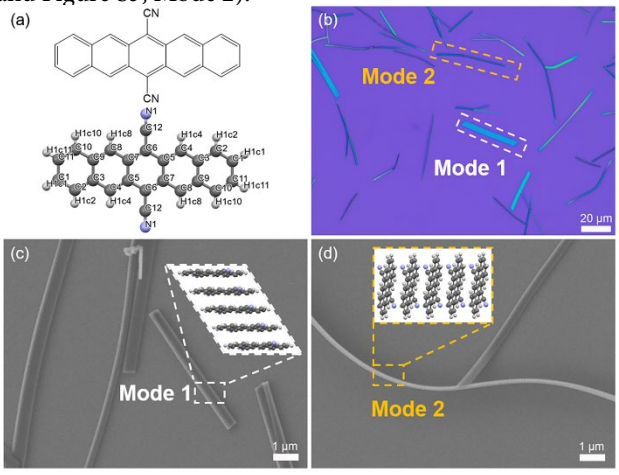

Figure 1 (a) Molecular structure of DCP. (b) Optical micrograph and (c–d) SEM images of micrometer-sized DCP crystals obtained using the PVT method (inset: top view of the corresponding molecular packing).

As reported in our previous work, DCP crystallized into a triclinic system in space group $P\bar{1}$ with the unit-cell parameters of a = 3.7935(7) Å, b = 9.9695(16) Å, c = 10.6808(17) Å, α = 100.729(5)°, β = 98.815(5)°, and γ = 100.671(5)° (Table S2, ESI†) [20]. Figures 2a and c show that DCP molecules formed an 1D infinite offset face-to-face stacking along the a-axis, with a parallelly slipped distance of 1.748 Å, a centroid-to-centroid distance of 3.793 Å (Figure S4, ESI †), and a short π–π stak-

ing distance of 3.366 Å. The incorporated cyano groups at the 6 and 13-positions of the pentacene skeleton prevent the C–H···π interactions and enhance the π–π interactions between adjacent molecules owing to the large steric hindrance effect, thus leading to a 1D slipped stacking motif that is very different from the herringbone packing motif without π–π overlap in pentacene crystals (wherein C-H···π interactions dominate the molecular arrangement) [1-2, 6]. Furthermore, the polar cyano groups can also introduce the C-H···N bonds (length: 2.666 Å; angle: 166.09°) between the neighboring π–π stacking columns in the direction of the *b*-axis (Figure 2b), providing a stable and ordered 1D slipped

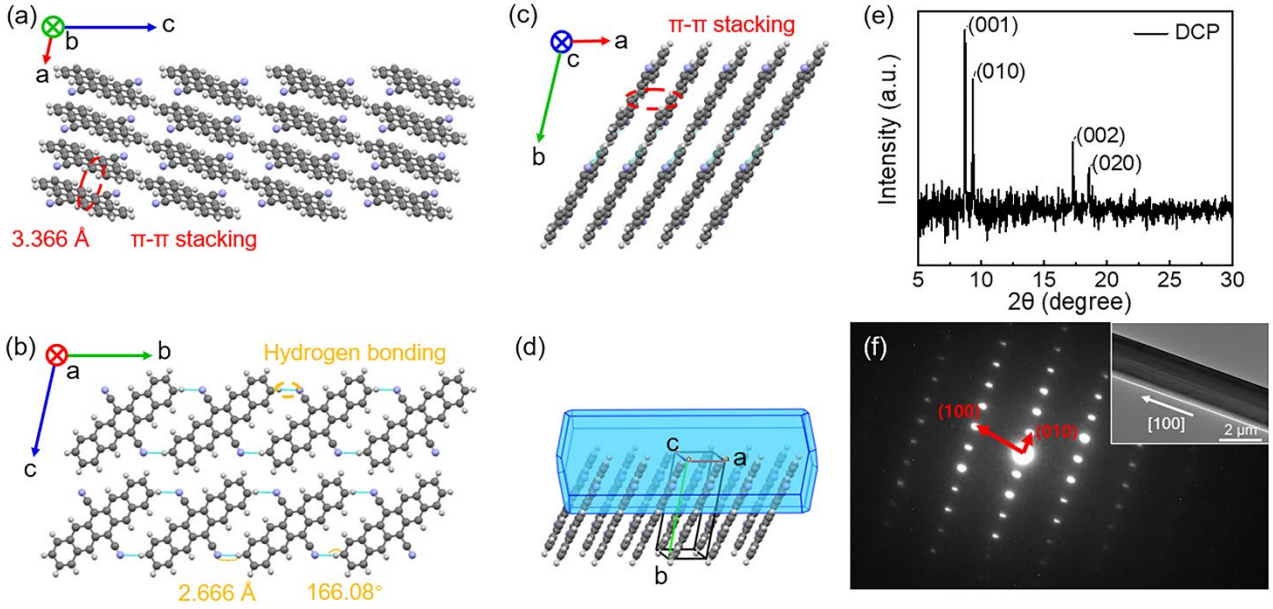

Figure 2 (a–c) Molecular packing in DCP single crystals. (d) BFDH morphology prediction for DCP single crystals. (e) PXRD patterns of the DCP micro/nano-structures grown on SiO_2/Si substrate. (f) TEM image and its corresponding SAED patterns of DCP 1D-MNMs in Mode 1.

stacking in the DCP crystal. The growth morphology of DCP crystals predicted by the Bravais–Friedel–Donnay–Harker (BFDH) model (Figure 2d) further illustrated that the DCP molecules aggregate into a ribbon-like morphology with the predominant growth direction along *a*-axis (π–π stacking direction) and the secondary dominant direction along the *b*-axis (hydrogen interactions), indicating that π–π interaction and hydrogen bonding are the main driving forces for DCP crystal formation [30].

Moreover, powder X-ray diffraction (PXRD), transmission electron microscopy (TEM), and selected area electron diffraction (SAED) analysis were performed to further reveal the molecular packing in DCP-based 1D-MNMs on OTS-modified SiO_2 substrates. As depicted in Figure 2e, the four distinct diffraction peaks at 2θ of 8.62°, 9.26°, 17.2°, and 18.5° found in the PXRD analysis can be assigned to the (001), (010), (002), and (020) crystal planes, respectively. These peaks indicate the two types of molecular orientations with either the *ab* plane or the *ac* plane parallel to the substrates, which agrees with the aforementioned different crystal growth modes (Figure 1). The TEM image and the SAED pattern for the lying-down microribbon-like DCP crystal are shown in Figure 2f, which were indexed to lattice constants that are the same as in the above single-crystal data. It can be inferred that, the DCP microribbon grows along the [100] direction, which coincides with the π–π stacking of DCP molecules (Figure 1c inset). In the same way, combined with the PXRD analysis (Figure 2e), we can predict that Mode 2 also grows preferentially along the [100] direction but with a different normal plane (Figure 1d inset). Moreover, the uniform morphology over the entire selected area with bright and clear diffraction spots in SAED images confirms the high crystallinity of DCP-based 1D-MNMs grown using the PVT method. The π–π stacking along the preferential growth direction of the DCP microribbon suggests that a favorable charge transport path can be achieved along the long axis of the DCP-based 1D-MNMs.

Consequently, we fabricated top-contact bottom-gate (TCBG) SCFETs to investigate the charge transport prop-

erties along the long axis of the DCP-based 1D-MNM, as shown in Figure 3a [31]. The SiO_2 surface was passivated by a monolayer of OTS to reduce the trap density induced by water and oxygen at the dielectric/semiconductor interface [32]. To investigate whether this can balance the hole and electron carrier injection, we chose either silver (work function of −4.26 eV) or gold (work function of −5.10 eV) as source/drain (S/D) electrodes (Figure 3b). First, the electrical characteristics of lying-down (Mode 1) microribbon crystals were investigated. As depicted in Table 1 and Figure S5–S6, when applying Ag as the S/D electrodes, the work function (−4.2 eV) being more aligned with the LUMO level (−4.16 eV) than the HOMO level (−5.87 eV) resulted in an unbalanced ambipolar transport with much higher electron transport (μ_e: 0.20 $cm^2\ V^{-1}\ s^{-1}$) than hole transport (μ_h: 0.06 $cm^2\ V^{-1}\ s^{-1}$) in a N_2 glove box. To improve the hole transport ability toward a balanced hole and electron transport, gold S/D electrodes were used to lower the hole injection barrier through better energy alignment with the HOMO level of DCP (Figure 3b). The corresponding SCFETs showed a well-balanced and improved ambipolar charge transport, with a maximum hole mobility of 0.38 $cm^2\ V^{-1}\ s^{-1}$ and electron mobility of 0.34 $cm^2\ V^{-1}\ s^{-1}$ (Table 1, Figure 3c–f, and Figure S5), which is among the best ambipolar transport characteristics achieved with 1D-MNMs [2-4, 9, 33-35]. Notably, compared with devices based on thin films (μ_e: ~10^{-4} $cm^2\ V^{-1}\ s^{-1}$, μ_h: 10^{-3}–10^{-4} $cm^2\ V^{-1}\ s^{-1}$), the mobility of SCFETs based on 1D-MNMs has been improved by more than two orders of magnitude [20]. Furthermore, the air stability was also investigated. Devices characterized in the ambient atmosphere (relative humidity of 44%) exhibited an increased hole mobility (μ_h: 0.46 $cm^2\ V^{-1}\ s^{-1}$) and a distinctly decreased electron mobility (μ_e: 0.03 $cm^2\ V^{-1}\ s^{-1}$). Different testing environments make different mobilities because electrons can be easily captured by atmospheric O_2 and H_2O and/or in the conducting channel. Therefore, the presence of O_2 and H_2O in ambient air usually results in an inferior and/or unstable electron transport [12]. Therefore, the electron mobility of the device measured in air is very low relative to the hole mobility. This phenomenon illustrates that the electron transport for our compound is very susceptible to O_2 and H_2O. However, the devices still exhibited relatively good air stability, with smooth test curves and almost no shift of the threshold voltage in repeated measurements (Table 1 and Figures S5 and S7).

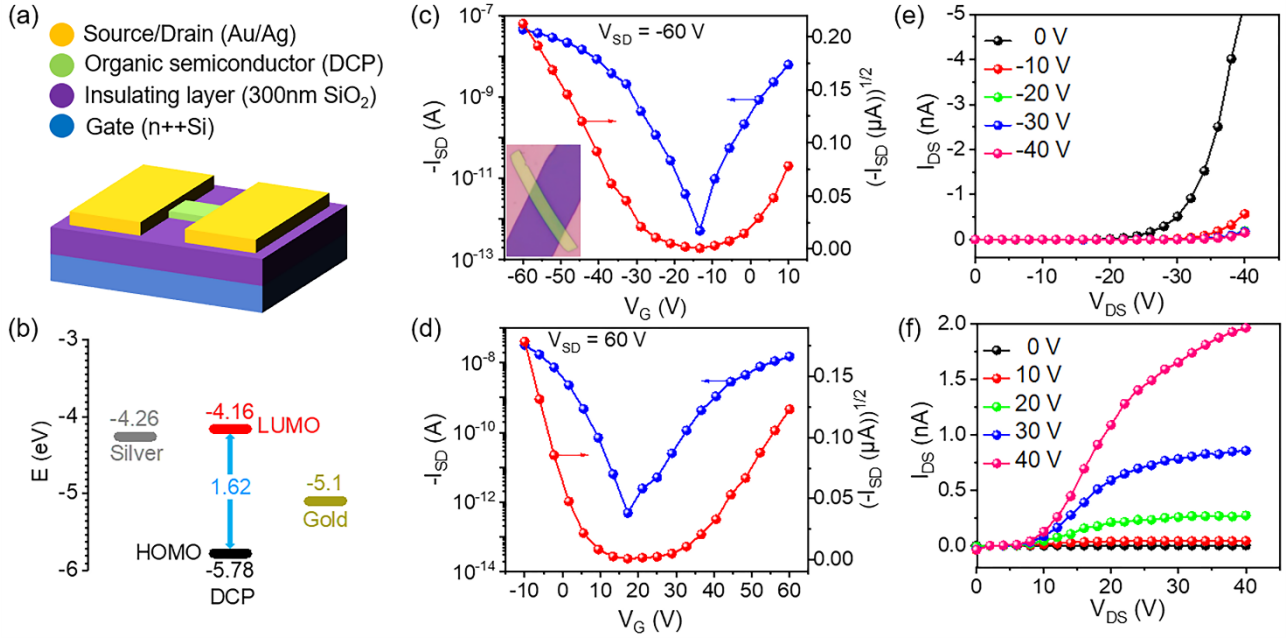

Figure 3 (a) Scheme of TCBG SCFETs based on DCP 1D-MNMs. (b) Diagram of the HOMO and LUMO energy levels of DCP relative to the work functions of Au and Ag contacts. (c, d) Typical transfer- and (e, f) output characteristics of SCFETs based on Mode 1 DCP single crystals with gold as S/D electrodes in N_2 atmosphere. (Inset: the corresponding device image).

Table 1 Electrical characteristics of SCFETs based on DCP 1D-MNMs.

Cpd.	Drain/Source Electrodes	Atmosphere	Mobility (Max/Ave) /cm^2 V^{-1} s^{-1}	V_T/V	On/Off ratio
Mode 1	Ag	N_2	μ_e=0.20/ 0.06	10 ~ 35	10^2 ~ 10^6
			μ_h=0.06/ 0.02	-20 ~ -50	10^2 ~ 10^3
	Au	N_2	μ_e=0.34/ 0.05	10 ~ 30	10^3 ~ 10^4
			μ_h=0.38/ 0.17	-10 ~ -40	10^3 ~ 10^4
	Au	Air	μ_e=0.03/ 0.005	10 ~ 30	10^2 ~ 10^3
			μ_h=0.46/ 0.15	-10 ~ -40	10^2 ~ 10^4
Mode 2	Au	Air	μ_e=2.76×10^{-4}/ 8.24×10^{-5}	20 ~ 60	10^3 ~ 10^4
			μ_h=0.18/ 0.05	-10 ~ -40	10^3 ~ 10^4

The devices exhibited a relatively long lifetime and good stability. As shown in Figure S8, even when devices with gold S/D electrodes were stored in air for over four months, their mobilities (μ_e = 0.013 cm^2 V^{-1} s^{-1}; μ_h = 0.013 cm^2 V^{-1} s^{-1}) did not decrease substantially compared with the initial device (μ_e = 0.035 cm^2 V^{-1} s^{-1}; μ_h = 0.028 cm^2 V^{-1} s^{-1}), nor did their on/off ratios (all devices measured in a N_2 atmosphere). The slight decrease in mobility and the increase in I_{off} may be due to the doped oxygen and/or water in 1D-MNMs and/or at the interface. Meanwhile, we also fabricated devices based on standing-up (Mode 2) microribbon crystals to explore their charge transport property. As displayed in Figure S9, the standing-up 1D-MNMs exhibited inferior charge transport characteristics compared to their lying-down counterpart: in the ambient atmosphere, the maximum electron mobility was only 2.76 × 10^{-4} cm^2 V^{-1} s^{-1} and the maximum hole mobility was 0.18 cm^2 V^{-1} s^{-1} (Table 1). The much lower ambipolar charge transport in Mode 2 1D-MNMs might result from the difficulty in charge carrier injection due to poor interfacial contact between S/D electrodes and standing-up microstructures.

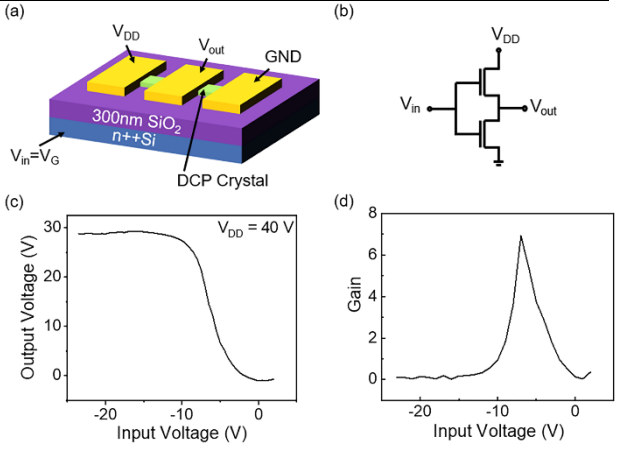

Figure 4 (a) Schematic illustration of a CMOS-like inverter comprising ambipolar transistors based on DCP 1D-MNMs. (b) Equivalent logical circuit diagram of the inverter. (c) Voltage-transfer characteristics and (d) the corresponding voltage gain of the inverter under the condition of V_{DD} = 40 V.

Finally, complementary inverters were constructed because of the balanced and excellent ambipolar charge transport of DCP-based 1D-MNMs (Mode 1). A 3D schematic diagram of the complementary inverter is displayed in Figure 4a, in which the ambipolar DCP-based 1D-MNM acted as the n- and p-channel semiconductors. As shown in Figure 4b, the corresponding logic circuit is composed of four electrodes: the top three gold contacts used to provide the operating voltage V_{DD}, monitor the output voltage V_{out}, and connect to the ground, respectively; their common back gate contact (silicon) served as the input voltage V_{in}. The voltage-transfer curve under V_{DD} = 40 V is shown in Figure 4c. V_{out} switches from a high voltage (V_{DD}) to a low voltage (~0 V) when V_{in} changed in a reversible way, verifying the function of the

complementary inverter [36-38]. Moreover, the voltage gain was calculated from the $V_{out} - V_{in}$ curve by taking the absolute value of the derivative of the voltage-transfer curve (dV_{out}/dV_{in}) [39-41]. As displayed in Figure 4d, the maximum calculated gain reaches up to 7, which is comparable to reported results [26, 42], indicating the potential application of the DCP-based 1D-MNMs in future logic circuits toward "molecular electronics" [27].

CONCLUSIONS

In summary, we have developed a novel ambipolar charge transporting 1D-MNM based on DCP with a 1D slipped stacking motif using the PVT method. Because of the strong π–π overlap in DCP-based 1D-MNMs and their well-matched energy level alignment with the electrodes, SCFETs showed excellent, well-balanced ambipolar charge transport behavior with a hole mobility of up to 0.38 $cm^2 V^{-1} s^{-1}$ and an electron mobility of up to 0.34 $cm^2 V^{-1} s^{-1}$ under nitrogen, which is one of the best ambipolar transport characteristics achieved for 1D-MNMs. In addition, the devices exhibited relatively good air stability, with smooth test curves and almost no shift in the threshold voltage in repeated measurements. Finally, a complementary inverter based on the DCP 1D-MNMs was constructed with a gain of up to 7, indicating potential application in future organic logic circuits. This work opens up the possibility of 1D-MNMs with a slipped stacking motif in the construction of ambipolar transistors.

Acknowledgements We are grateful for the Fundamental Research Funds for the Central Universities (buctrc202103, buctrc202128), the National Natural Science Foundation of China (52103200, 22171019, 21975263), SINOPEC (No. 222131), Open Funds of the State Key Laboratory of Optoelectronic Materials and Technologies (Sun Yat-sen University), State Key Laboratory of Luminescent Materials and Devices (2022-skllmd-14), State Key Laboratory of Supramolecular Structure and Materials (SKLSSM2022036).

Author contributions Zhen Y and Glöcklhofer F designed the project. Zhen Y, Shi C, and Wang Z guided the project. Wang Z, Hu Y, and Xie Y conducted the experiments. Wang Z and Hu Y wrote the manuscript. Zhen Y, Zhang L, Qie F, and Glöcklhofer F revised the manuscript. Guo J contributed to the experimental analysis. Wang Z, Hu Y, and Xie Y contributed equally to this article. All authors contributed to the general discussion.

Conflicts of interest The authors declare that they have no conflicts of interest.

Supplementary information Experimental details and supporting data are available in the online version of this paper.

Zongrui Wang is an associate professor at the Beijing University of Chemical Technology (BUCT). She received her Ph.D. degree from the Institute of Chemistry, CAS (ICCAS) in July 2016. From 2016 to 2021, she successively worked as a Research Fellow at the Nanyang Technological University, Singapore. In 2021, she joined BUCT as an associate professor. Her present research interest focuses on the molecular assembly of organic optoelectronic materials, flexible electronics, and transistor-based sensors.

Chunfeng Shi has been a professor at the Research Institute of Petroleum Processing (RIPP), SINOPEC, since 2015. He received his Ph.D. degree from RIPP and then worked as a researcher at RIPP in 2008. His research focuses on environmentally benign chemistry and nanomaterials chemistry, particularly for developments in green selective oxidation technology catalyzed by zeotype or carbon catalysts and the green preparation of nanomaterials.

Florian Glöcklhofer is a Research Fellow at Imperial College London. He received his Ph.D. degree from TU Wien (Vienna) in 2017 and moved to Imperial College London on a Marie Skłodowska-Curie Individual Fellowship in 2018. His research focuses on the design and synthesis of π-conjugated macrocycles for battery electrodes and other applications as well as the development of new synthetic approaches to aromatic compounds.

Yonggang Zhen is a professor at the Beijing University of Chemical Technology (BUCT). He received his Ph.D. degree from the Institute of Chemistry, CAS (ICCAS) in 2010. Then, he worked as a postdoc researcher at the University of Tokyo. He returned to ICCAS in 2013 and moved to BUCT in 2021. His research focuses on the synthesis, self-assembly, and crystal engineering of organic optoelectronic materials as well as the preparation of flexible electronic materials and devices.

基于6,13-双氰基并五苯一维滑移堆积微米带状晶体的双极性电荷传输

王宗瑞[a*†], 胡洋[a†], 谢玉洁[a†], 郄凤翔[b], 郭俊峰[a,c], 张磊[a], 史春风[b*], Florian Glöcklhofer[d*], 甄永刚[a,e*]

摘要 基于有机π共轭体系的一维自组装微纳米材料(1D- MNMs)具有较少的散射电荷传输、尺寸适中、易于制备等优点，可以方便地构筑集成微电路。虽然基于p沟道或n沟道有机半导体的一维自组装微纳米材料已经取得了巨大的进展，但遗憾的是，迄今为止，基于双极性有机半导体的一维自组装微纳米材料还非常缺乏。本文利用物理气相传输法，制备了基于6,13-双氰基并五苯(DCP)一维滑移堆积的新型一维自组装微纳米材料，表现出良好的双极性电荷传输特性，电子和空穴迁移率分别达到0.34和0.38 $cm^2 V^{-1} s^{-1}$，是一维自组装微纳米材料中最好的双极性电荷传输特性之一。此外，基于双极性DCP的一维自组装微纳米材料构建了互补型反相器，增益可达7，表明其在有机逻辑电路中具有潜在的应用前景。